IOP Conf. Series: Materials Science and Engineering **226** (2017) 012147 doi:10.1088/1757-899X/226/1/012147

Flow Characteristics Near to Stent Strut Configurations on Femoropopliteal Artery

Muhammad Sufyan Amir Paisal[1*], Syed Fadhil Syed Adnan[1], Ishkrizat Taib[1], Al Emran Ismail[1], Mohammad Kamil Abdullah[1], Normayati Nordin[1], Suzairin Md Seri[1], Nofrizalidris Darlis[2]

[1]Flow Analysis, Simulation and Turbulence Research Group, Faculty of Mechanical and Manufacturing Engineering, Universiti Tun Hussein Onn Malaysia, Parit Raja, 86400 Batu Pahat, Johor, Malaysia.
[2]Faculty of Engineering Technology, Universiti Tun Hussein Onn Malaysia, Parit Raja, 86400 Batu Pahat, Johor, Malaysia.

Corresponding author: muhammadsufyanamir@gmail.com

Abstract. Femoropopiteal artery stenting is a common procedure suggested by medical expert especially for patient who is diagnosed with severe stenosis. Many researchers reported that the growth of stenosis is significantly related to the geometry of stent strut configuration. The different shapes of stent geometry are presenting the different flow pattern and re-circulation in stented femoropopliteal artery. The blood flow characteristics near to the stent geometry are predicted for the possibility of thrombosis and atherosclerosis to be formed as well as increase the growth of stenosis. Thus, this study aims to determine the flow characteristic near to stent strut configuration based on different hemodynamic parameters. Three dimensional models of stent and simplified femoropopliteal artery are modelled using computer aided design (CAD) software. Three different models of stent shapes; hexagon, circle and rectangle are simulated using computational fluid dynamic (CFD) method. Then, parametric study is implemented to predict the performance of stent due to hemodynamic differences. The hemodynamic parameters considered are pressure, velocity, low wall shear stress (WSS_{low}) and wall shear stress (WSS). From the observation, flow re-circulation has been formed for all simulated stent models which the proximal region shown the severe vortices. However, rectangular shape of stent strut (Type P3) shows the lowest WSS_{low} and the highest WSS between the range of 4 dyne/cm^2 and 70 dyne/cm^2. Stent Type P3 also shows the best hemodynamic stent performance as compare to others. In conclusion, Type P3 has a favourable result in hemodynamic stent performance that predicted less probability of thrombosis and atherosclerosis to be formed as well as reduces the growth of restenosis.

1. Introduction

Recently, stents has been used widely in the treatment of narrowed artery which is called stenosis. Stenosis is one of the factors in peripheral arterial disease (PAD) that occurred when a lipids or fats such as cholesterol being deposited into the artery wall and making it rigid. It can be treated by using stent to widen the narrowed artery. However, previous study reported that restenosis might be occurred after a few weeks of the stenting procedure. The growth of restenosis is significantly related to hemodynamic effects on the stent strut configuration [1][2]. The hemodynamic parameters that play the important role in development of stenosis are wall shear stress (WSS), low wall shear stress (WSS_{low}), velocity and pressure. The changes in WSS induced by an implanted stent play a significant role in the immunological behaviour of the femoropopliteal artery [3]. This behaviour is directly linked to restenosis within the stented artery. The experts predicted that the stent strut geometry had a major contribution of restenosis process, especially on the formation of thrombosis and atherosclerosis. Even though stent strut geometry plays such a key role in the restenosis process, it has relationship with the WSS distribution near the stent strut geometry [4].

Numerical computational modelling has appeared as an important tool for the studying of different geometrical stent struts such as circular, rectangular and hexagonal cross-section shape. Such models could give better optimization result of stent strut geometry than the benchmarked model. In 2016, Yongfei *et al* stated that the use of the computational fluid dynamics (CFD) methods could predict the potential risk of restenosis and wall shear stress distribution in stented arteries [5]. Some computational models were developed with various modelling setup such as 3D stented artery mode versus axisymmetric parallel ring, compressible flow versus incompressible flow, pulsatile flow versus steady-state and Newtonian versus non-Newtonian. Therefore, computational modelling is suitable to investigate the influence of stent geometry onto the hemodynamic of artery [6][7].

This study offers a detail statistical data distribution in predicting the hemodynamic performance among the stents. Furthermore, the study is also conducted in order to pre-clinically evaluate the stent impact on the femoropopliteal artery stenting. This study also compares the hemodynamic variable effects on three different cross-sectional areas with same size and shape of benchmarked stent. The hemodynamic variables included are WSS, WSS_{low}, velocity and pressure. Thus, this analysis goal is to predict the hemodynamic stents performance through CFD method to decrease the development of restenosis.

The development of restenosis is influenced by the flow disturbance near to the stent strut configuration [8][9][10][11]. The development of atherosclerosis for the WSS_{low} is predicted to be less than 4 dyne/cm². The prediction for WSS greater than 70 dyne/cm² can lead the formation of thrombosis [12][13]. Hence, the data of WSS are measured near to the arterial wall and stent surface.

For summary, flow disturbance or re-circulation has been found near to the stent strut configuration which is increasing the possibility of restenosis process. The restenosis growth could be reduced by selecting stent configuration with better flow characteristic. Thus, this study is focusing on flow characteristic near to arterial wall stenting due to different geometry of stent strut configuration.

2. Methodology

2.1. The simplified model of femoropopliteal artery

The model of femoropopliteal artery is modelled in a straight model as shown in Figure 1(a). This model is simplified based on the work done by previous researchers as shown in Figure 1 (b) into a straight cylindrical shape with no stenosis as shown in Figure 1(a) [14][15]. The simplified model is simulated to provide the fundamental knowledge of flow behaviour and its effect on the implantation of stent in femoropopliteal artery. Three different cross-sectional areas of stent strut configuration are taken into consideration. The diameter (D) of femoropopliteal artery has 6 mm and the length (L) of artery is 40mm as shown in Figure 1(a).

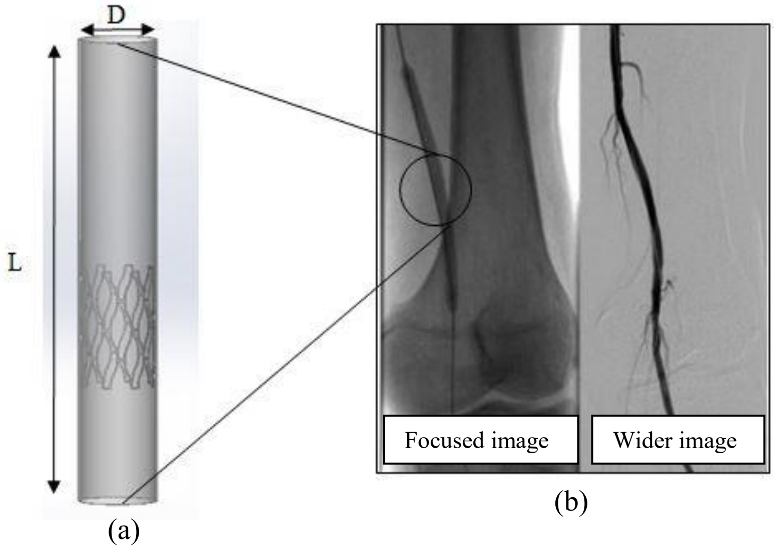

Figure 1. (a) Illustration of simplified straight femoropopliteal artery. (b) Patient specific femoropopliteal artery model taken from angiogram focusing on balloon post-dilation of the stent (left) and a wider image of patient artery (right) [15].

2.2. Strut configuration and geometrical shape of stent

Three different types of stent are modeled consist of benchmarking stent and two modified stents. The selected benchmarking stent is Type P1 and the other two modified stents are Type P2 and Type P3. Two types of stent strut configurations that have been used are opened type cell and closed type cell. Opened type cell design shows the removal of linkage between each strut while closed cell shows the linkage. In this study, Type P1 and Type P2 is opened type cell while Type P3 is closed type cell which can be seen in Table 1.

Detail information of stent strut configuration consisting of different types of strut cell and linkage along with the number of slots per unit cell is shown in Table 2. In varying the geometrical shape of stent, the cross-sectional shape of stent is classified into three different shapes which are rectangle, circle and hexagon as seen in Table 3. The length (L_S) of stent is 10 mm, the outer diameter (D_o) is 6 mm and the inner diameter (D_i) is 5.8 mm as shown in Figure 2.

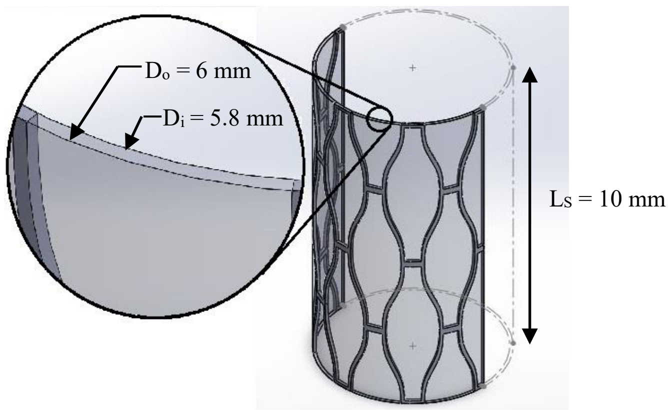

Figure 2. Dimension of stent Type P1.

Table 1. Illustrations of benchmarking stent Type P1 and improved stent Type P2 and Type P3.

Type P1	Type P2	Type P3
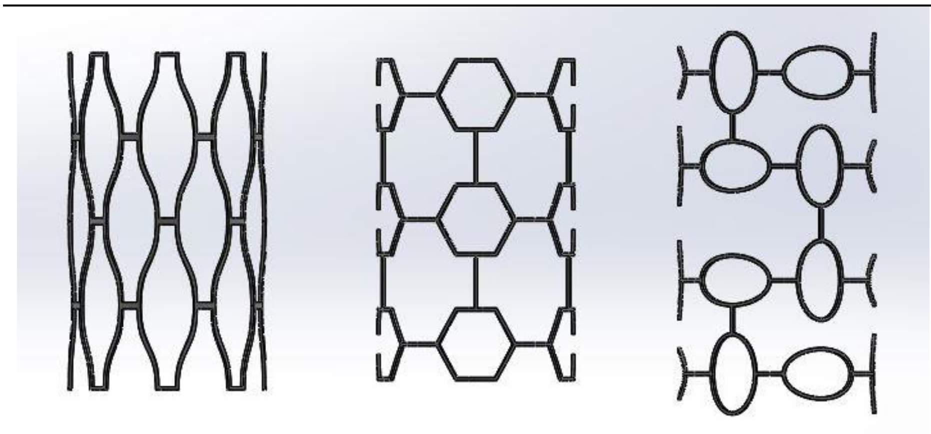		

Table 2. Detail information of stent strut configuration.

No	Type of Stent	Link structural type	Type of cell	Pattern of shape	Number of slot (per unit cell)
1	Type P1	No connector	Closed	Repeated shape	16
2	Type P2	Bend shape link	Closed	Hexagon shape	10
3	Type P3	Bridging	Opened	Ellipse shape	12

Table 3. Cross-sectional shapes of stent strut configuration for Type P1.

Rectangle	Hexagon	Circle
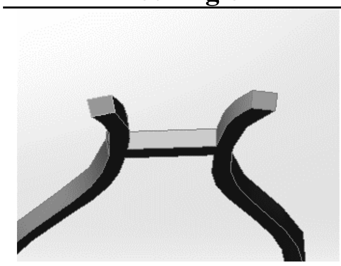	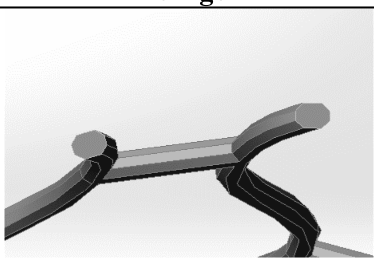	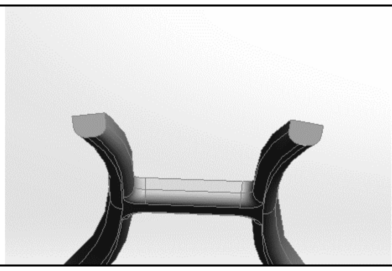

2.3. Meshing of stented femoropopliteal artery model

A computational domain of simplified femoropopliteal artery model implanted with three types of stents is drawn by using CAD software SOLIDWORKS 2015 (Dassault Systemes Solidworks Corporation, Waltham, MA) and then transferred into ANSYS CFX 16.1 (Canonsburg, PA, USA) for discretization process. The computational domain is generated into tetrahedral mesh as shown in Figure 3. The tetrahedral mesh is considered because of complexity of the stent model and it is required to gain two point nodes between fluid domain and wall domain. To obtain the best result, the finest meshing is applied near to stent strut configuration. However, fine mesh requires high computational time. Thus, a grid independence test is conducted to get optimum mesh quality without affecting much of the resulting analysis.

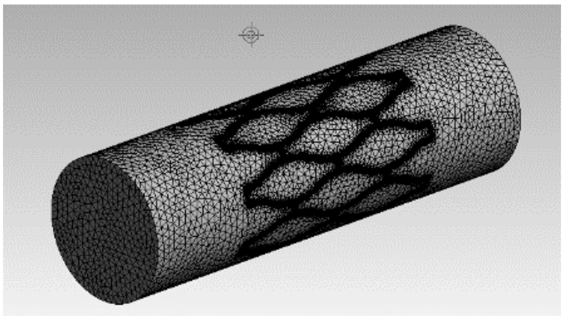

Figure 3. Tetrahedral mesh of the computational domain.

2.4. Parameter assumptions and boundary conditions

Blood is assumed as incompressible and Newtonian fluid which the shear rate is larger than 100 per second. It has an average density of approximately 1060 kg/m^3 and dynamic viscosity of 0.0035 kg/ms [16]. The blood vessel is assumed to be rigid and no slip condition between stents and blood vessel [5]. The boundary condition for inlet and outlet is shown in Figure 4. Steady flow is considered into the analysis of hemodynamic effect on different strut cross-sectional area. The inlet velocity and outlet pressure is shown in Table 4 with three pulsating cardiac phases [17][18][19][20].

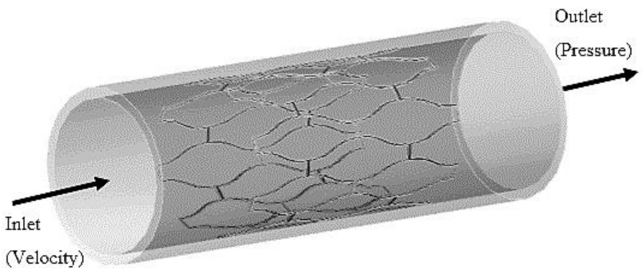

Figure 4. Boundary conditions of stented femoropopliteal artery model.

Table 4. Velocity inlet and pressure outlet assigned in boundary condition of femoropopliteal artery according to the cardiac phase [19][20].

Cardiac phase	Velocity (m/s)	Pressure (Pa)
Peak Systolic	0.50	21731
Late Diastolic	0.05	10532
Mean	0.10	14590

2.5. Computational model and governing equations

ANSYS CFX 16.1 is used in solving the simulation using finite volume method which representing and evaluating the governing equations spatially on computational mesh. The pressure outlet and velocity inlet are computed to solve the continuity and Navier-Stokes equation. The blood flow in the computational domain is governed by the following incompressible Navier-Stokes equation:

$$\nabla \cdot V = 0 \tag{1}$$

$$\rho \frac{DV}{Dt} = -\nabla P + \mu \nabla^2 V \tag{2}$$

Where ρ is blood density, P is blood pressure, μ is viscosity of blood and V is blood flow velocity.

3. Result and Discussion

3.1. Grid Independence Test

Figure 5 shows the result of velocity profile for stented femoropopliteal artery models with different number of nodes which are 954k, 965k, 1009k and 1350k. The selection of node is based on an unchanging result of the parameter with respect to the increasing number of node. For this simulation, 1009k node is chosen because of the resulting velocity is almost identical to the 1350k node.

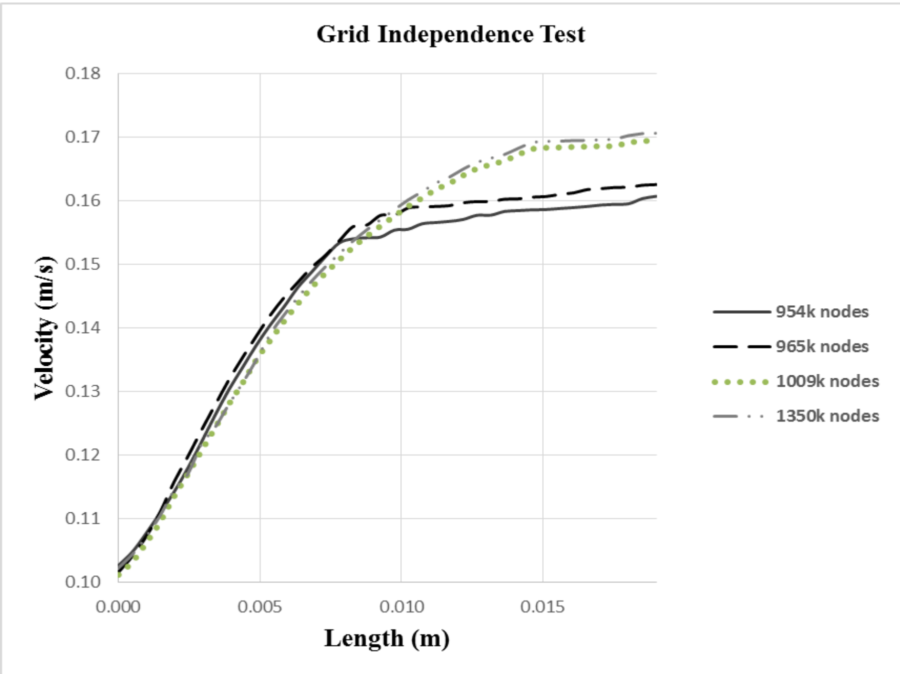

Figure 5. Velocity distributions at the centre of femoropoptelial artery for different meshing.

3.2. Wall shear stress (WSS)

The development of stenosis process is influenced by the design of stent strut configuration. The main factors that influence the growth of stenosis are thrombosis and atherosclerosis. The formation of thrombosis and atherosclerosis can be predicted numerically based on hemodynamic factors; WSS and WSS_{low}. The development of atherosclerosis is predicted for WSS_{low} value to be lower than 4 dyne/cm^2. However, the WSS value which is greater than 70 dyne/cm^2 could lead to the formation of thrombosis [13]. In this study, WSS distribution is simulated into three different cardiac phases; peak systolic (the highest blood pressure), late diastolic (the lowest blood pressure) and mean (average arterial blood pressure) as shown in Table 4.

At late diastolic time, the lowest value of WSS_{low} is 0.1 Pa for Type P1 with rectangular shape of strut cross-section while the maximum value of WSS is 1.82 Pa for Type P2 and P3 with circular shape of strut cross-section. However, mean of cardiac phase shows that Type P3 with rectangular shape of strut cross-section has the lowest WSS_{low} which is 0.236 Pa while Type P3 with circular cross-sectional shape of strut has the highest WSS value which is 4.7 Pa. At the peak systolic of cardiac phase, the minimum value of WSS_{low} is 2.8 Pa for Type P2 and P3 with rectangular shape of strut cross-section while the maximum value of WSS is 65 Pa by Type P3 with circular shape of strut cross-section.

In overall, the improved stents have WSS distribution which is not passing beyond 70 dyne/cm^2 that induce the thrombosis formation. However, the selection of the best stent still needs to be in precaution since some of the stents have WSS_{low} distribution that is in the range for high possibility of atherosclerosis formation. After taking the WSS_{low} value into consideration, the most suitable stent strut configuration among the studied stents for femoropopliteal artery is Type P3.

The design of stent strut also plays a main role in controlling the WSS distributions. Table 6 shows the different WSS distribution by stent Type P3 for each shape of the cross-section at the cardiac phase of peak systole which; rectangular shape has 28 Pa of WSS and 2.8 Pa of WSS_{low}; circular shape has 65 Pa of WSS and 6.5 Pa of WSS_{low}; hexagonal shape has 59 Pa of WSS and 5.9 Pa of WSS_{low}. Qualitatively and quantitatively, the most incomparable cross-sectional strut design among the three shapes is the rectangular shape that has less area with high WSS and low WSS_{low} distribution along with the most minimum WSS distribution. This is due to other shapes that have more area with high WSS value and low WSS_{low} value. More WSS_{low} distribution shows the design to have WSS near to zero indicating that there is a stagnation flow. The blood flow should not to be stagnant in the artery because it increases the probability to have the formation of atherosclerosis.

Table 5. Distributions of WSS in stented femoropopliteal artery.

Stent			Cardiac phase		
Case	Type	Shape	Peak systolic	Late diastolic	Mean
a	P1	Rectangle			
b	P1	Circle			
c	P1	Hexagon			
d	P2	Rectangle			
e	P2	Circle			
f	P2	Hexagon			
g	P3	Rectangle			
h	P3	Circle			
i	P3	Hexagon			

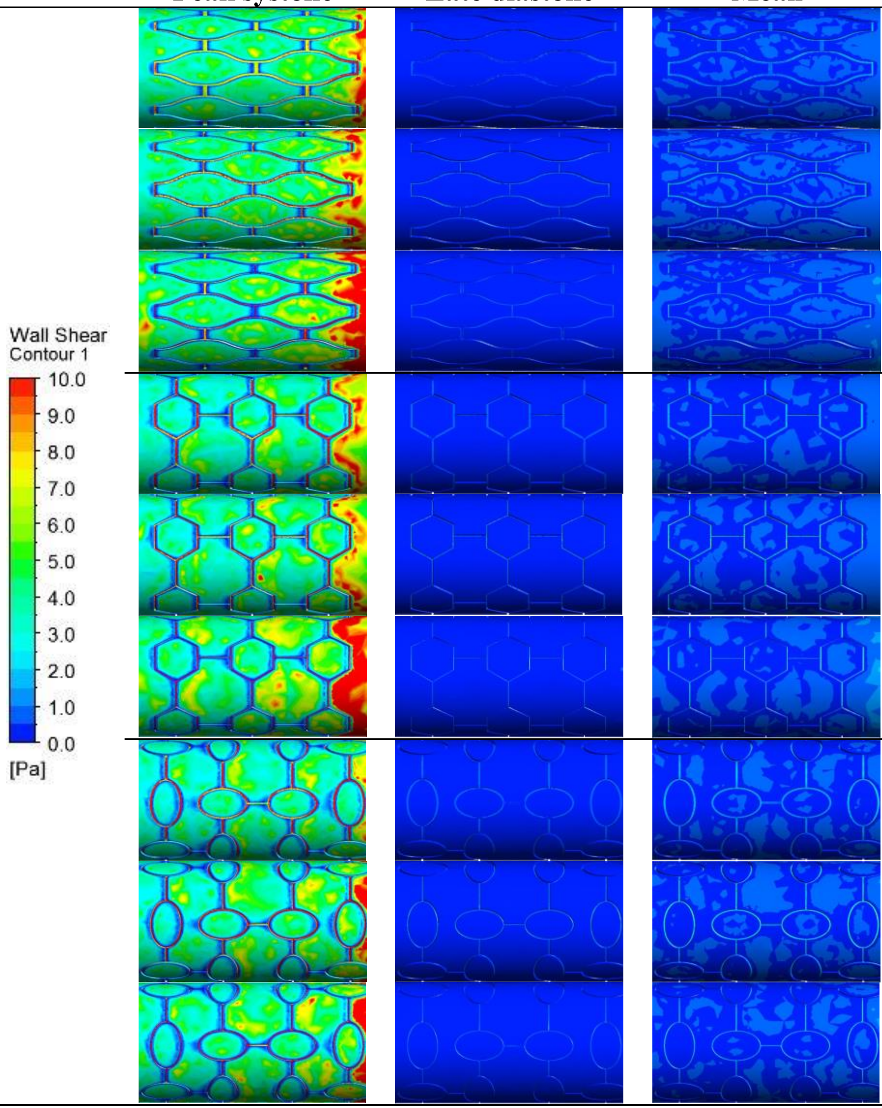

Table 6. Distribution of WSS varying to the strut cross-sectional shape of Type P3 at peak systolic.

Shape		WSS distribution
Rectangle	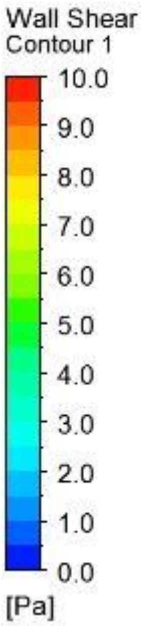	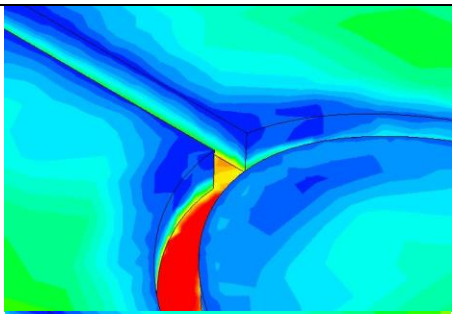
Circle		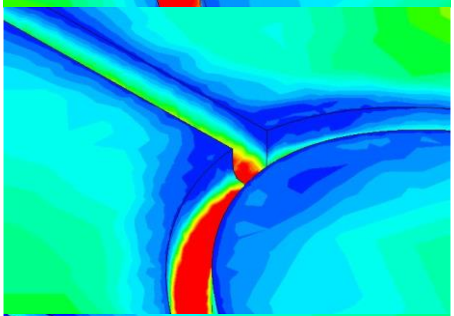
Hexagon		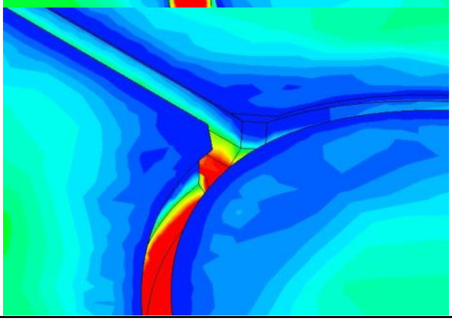

3.3. Velocity and Pressure

The shapes of the strut cross-section also give an effect to the hemodynamic parameters of velocity and pressure distributions. Figure 6 and Figure 7 have proved that the varying velocity and pressure distributions of the stated hemodynamic parameters which the highest velocity is rectangular strut, followed by circular and hexagonal strut. The pressure change for all shapes of the strut is almost identical as the pressure becomes lower in the length of 0.025 m distance from proximal.

However, the most critical change for both pressure and velocity is the shape of hexagonal strut. This kind of shape should not be used in the future work due to its shape that gives abnormal pressure curve compared to other shapes and also traps more blood flow between the arterial wall and the stent.

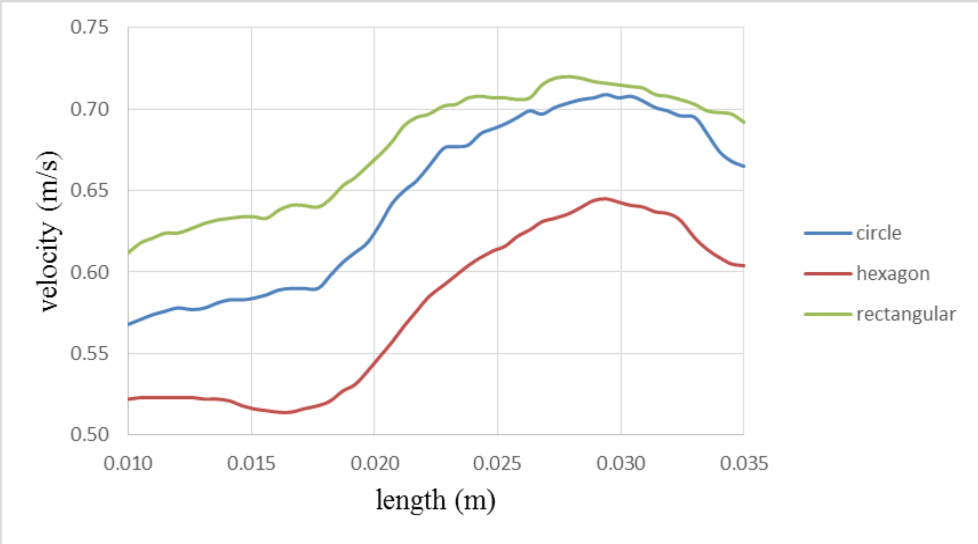

Figure 6. Velocity distributions along the computational domain of stent Type P3 at peak systolic.

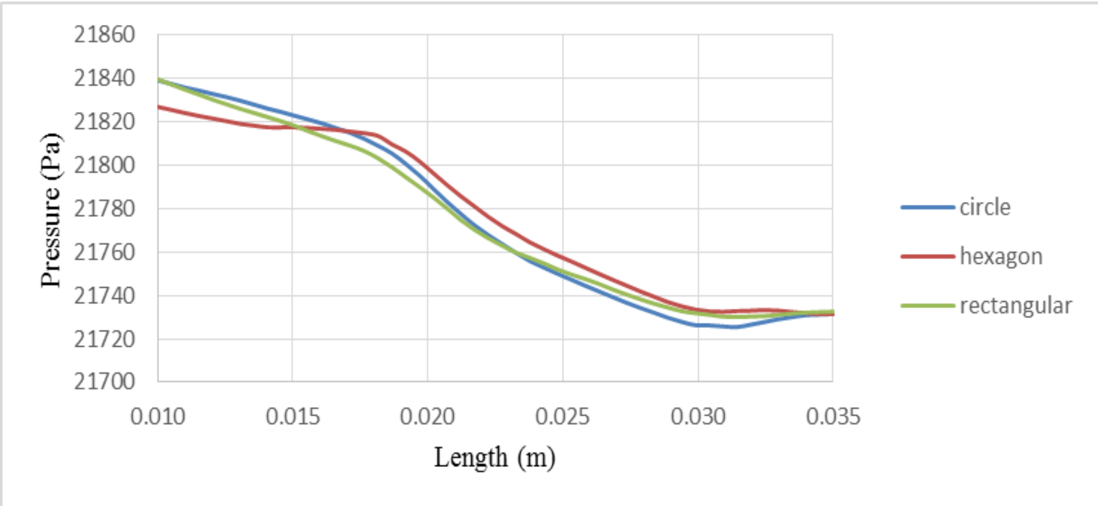

Figure 7. Pressure distributions along the computational domain of Type P3 at peak systolic.

3.4. Blood Flow Re-Circulation

The blood flow re-circulation near the stent strut is indicated by viewing the streamline and 2-D vector plot of velocity parameter. However, all types of the stent cross-sectional shape give different results of re-circulation. The visibility of re-circulation for both streamline and vector plot becomes clearer and higher from the increasing order of rectangle, circle and hexagon shape of the cross-sectional stent strut as shown in Table 6. A high re-circulation of the blood flow could increase the possibility of thrombosis to be formed. Thus, the hexagon shape has higher possibility of thrombosis formation compared to the circle and rectangle shape.

Table 6. Streamline and 2-D vector plot of blood flow near to the strut cross-sectional shape of P3 stent at peak systolic.

Shape	Streamline	2-D vector plot
Rectangle	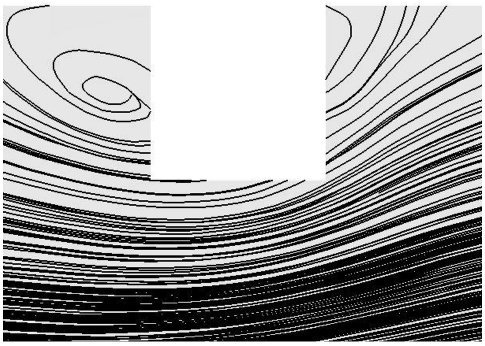	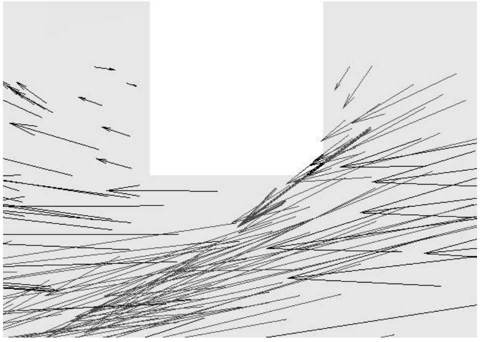
Circle	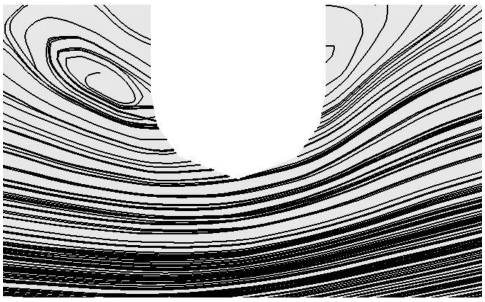	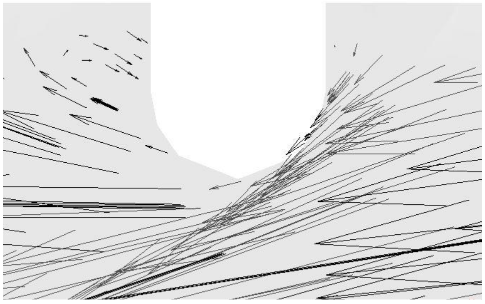
Hexagon		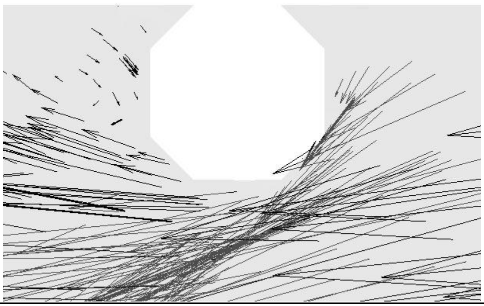

4. Conclusion

The stent models show the varying flow characteristics near to the strut configuration. In general, all stented model of femoropopliteal artery have not reached the maximum value of WSS. Nevertheless, the rectangular shape of the Type P3 strut shows the lowest value of WSS_{low} and the highest WSS value which is in normal arterial range between 4 dyne/cm^2 and 70 dyne/cm^2. The design model of Type P3 also shows the best hemodynamic stent performance in term of WSS distribution as compared to other type of stents.

Based on the analysis that has been made on the shape of stent strut cross-section, hexagon shape gives the highest wall shear stress, high blood flow re-circulation, unstable low velocity and abnormal pressure distribution. Thus, the circular and rectangular struts are the essential shapes to be chosen for low risk of restenosis especially the thrombosis and atherosclerosis formation.

Acknowledgement

The support of the University Tun Hussein Onn Malaysia, under the GPPS grant project, led by Dr. Ishkrizat Taib and under grant number **U723** is gratefully acknowledged. This paper was partly sponsored by the Centre for Graduate Studies UTHM.

References

[1] Balossino R, Gervaso F, Migliavacca F and Dubini G 2008 *J. Biomech.* **41** 1053–1061.
[2] Sullivan T M, Ainsworth S D, Langan E M, Taylor S, Snyder B and Cull D 2002 *J. Vasc. Surg.* **36**(1) 143–149.
[3] Garasic J M , Edelman E R, Squire J C, Seifert P, Williams M S and Rogers C 2000 *Circulation* **101** 812–819.
[4] Hsiao H, Lee K, Liao Y and Cheng Y 2012 *Micro Nano Lett.***7**(3) 430–433.
[5] Yongfei J, Jun Z and Wanhua Z 2016 *Chinese J. Mech. Eng.* **29** 1–9.
[6] Murphy J B and Boyle F J 2010 *Biorheology* **00** 1–16.
[7] Gao X W, Cheng H-D, and Brebbia C A 2013 *Boundary Elements and Other Mesh Reduction Methods XXXVI* (Ashurst: WIT Press).
[8] Kastrati A, Mehilli J, Dirschinger J, Seyfarth M and Schmitt C 2001 *Am. J. Cardiol.* **87** 34–39.
[9] Chiu J and Chien S 2013 *Physiol Rev.* **91**(1) 1–106.
[10] Jiménez J M and Davies P F 2010 *Ann Biomed Eng.* **37**(8) 1–24.
[11] Balakrishnan B, Tzafriri A R, Seifert P, Groothuis A, Rogers C and Edelman E R 2005 *Circulation* **111** 2958–2965.
[12] Kim B J, Ha H, Huh H K, Kim G B, Kim J S, Kim N and Lee S 2016 *J. Stroke* **18**(1) 66–72.
[13] Malek A M, Alper S L and Izumo S 1999 *Jama* **282**(21) 2035–2042.
[14] Khader S M A, Ayachit A, Raghuvir P B, Ahmed K A, Rao V R K and Kamath S G 2014 FSI Simulation of Increased Severity in Patient Specific Common Carotid Artery Stenosis *3rd International Conference on Mechanical, Electronics and Mechatronics Engineering (ICMEME'2014) March 19-20,2014 Abu Dhabi (USE)* pp 16–21.
[15] Diamantopoulos A and Katsanos K 2014 *Semin Interv. Radiol* **31** 345–352.
[16] Chandran K B, Yoganathan A P and Rittgers S E 2007 *Biofluid Mechanics The Human Circulation* (Boca Raton: Taylor & Francis).
[17] Kastrati A, Mehilli J, Dirschinger J, Seyfarth M and Schmitt C 2001 *Am. J. Cardiol.* **87**(1) 34–39.
[18] Puntawangkoon C, Kitzman D W, Kritchevsky S B, Hamilton C A, Nicklas B and Leng X 2009 *J. Cardiovasc. Magn. Reson.* **11** 1–11.
[19] Chakravarthy M, Holla S, Gowda N, Anand A, Mattur K and Reddy K 2012 *Indian J. Anaesth.* **56**(1) 83–85.
[20] Delis K T, Nicolaides A N and Stansby G 2000 *Arch Surg.* **135**(3) 265–269.